NRIAG Journal of Astronomy and Geophysics (2013) **2**, 45–53

National Research Institute of Astronomy and Geophysics

NRIAG Journal of Astronomy and Geophysics

www.elsevier.com/locate/nrjag

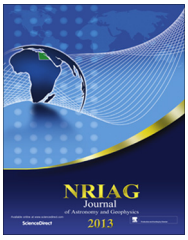

Time verification of twilight begin and end at Matrouh of Egypt

A.H. Hassan, N.Y. Hassanin, Y.A. Abdel-Hadi *, I.A. Issa

National Research Institute of Astronomy and Geophysics, Helwan, Egypt

Received 30 October 2012; accepted 30 January 2013
Available online 11 July 2013

Abstract Twilight observations were carried out in the period «1983–1985» in different seasons at different sites mainly to deduce the beginning and the end of twilight. One of these sites was Matrouh. These observations were gathered using a refractor (an alt-azimuth scanner) of 10 cm diameter associated with a photoelectric tube of the type ($\varphi \rightarrow Y - 51$) using 3-filters namely; the blue, visual and red filters. The photoelectric system was calibrated with the international photoelectric color system. The phenomena were followed in steps each 10° in both altitude and azimuth. The depression of the sun below the horizon was calculated from the local time of each scan. The results indicated (at $a = 5°$ and $A = 10°$) for the latitude of Matrouh that the end and the beginning of the twilight occurred when the depression of the sun (D_o) was between 18° and 20°, while the dawn times were found to be between 14° and 16°. The brightness of the twilight phenomena was followed, however, to different altitudes and azimuths [$0° \leqslant a° \leqslant 60°$ and $0° \leqslant A° \leqslant 60°$].

1. Introduction

Along with the researches of Issa and Hassan (2008a,b,c, 2011) and what was mentioned therein regarding the main aim of this project, which was supported by Al-Azhar, Dar El-Iftaa and the Academy of Scientific Research and Technology in Egypt and executed by the National Research Institute of Astronomy and Geophysics (NRIAG), we proceed further to give and discuss the begin and the end of twilight at the third site, Matrouh in Egypt (Lat. = 31°0.2′N, Long. = 27°51′E, Elev. 75 m). For more details and literature see papers I, II and III (Issa and Hassan, 2008a,b,c) and Issa and Hassan (2011).

1.1. Weather parameters at Matrouh

Weather parameters are given in Table 1 below including pressure (mb), relative humidity, *R.H.* (%), and temperature, *T* (°C). In summer for the period May 4–7, 1984, the climate status at Matrouh is summarized in Table 2. At the end of twilight, dispersed white clouds have been noticed at altitude 5–10°. On May 5, heavy black clouds are observed at 30° altitude. On May 7, heavy white clouds have been noticed between 25° and 30° altitude and water vapor is observed. In summer (June 1–6), clear sky with no clouds was dominating. Sometimes heavy fog moved in the region of observations.

* Corresponding author. Mobile: +20 1000556473.
E-mail address: yasser_hadi@yahoo.com (Y.A. Abdel-Hadi).
Peer review under responsibility of National Research Institute of Astronomy and Geophysics.

ELSEVIER Production and hosting by Elsevier

2090-9977 © 2013 Production and hosting by Elsevier B.V. on behalf of National Research Institute of Astronomy and Geophysics.
http://dx.doi.org/10.1016/j.nrjag.2013.06.008

Table 1 The meteorological conditions in summer at Matrouh.

Evening			Morning		
Pressure (mb)	*R.H.* %	*T* (°C)	Pressure (mb)	*R.H.* %	*T* (°C)
999.3	79.3	20.8	996	91	17

Table 2 The meteorological conditions in summer at Matrouh from the General Authority for Meteorology.

Weather parameters	Summer
Pressure reduced to M.S.L.	1012.6 mb
Relative humidity	68%
Surface temperature, (mean)	23.3 °C
Total rain fall, Tr	2 mm
Evaporation per day at 06 U.T.	8.4 L/day
Mean No. of days of occurrence of	
Haze (vis. < 1000 m)	0.80
Fog (vis. > 1000 m)	2.4
Mist (vis. > 1000 m)	0.3
Dust or sand rising > 1000 m	2.7
Dust or sand rising < 1000 m	0.3
Mean surface wind speed in knots (1 knot = 1.75 km/h)	10 knot
Cloudy (total sky coverage at U.T. 0600, 1800)	2, 1.6 Oktas

Also, Table 2 shows the same parameters for the same area recorded by the Egyptian General Authority for Meteorology. We can notice some slight differences in some values of the parameters, but it does not affect the accuracy of our recorded data significantly.

2. Method

However, for prayer time verification, we have limited ourselves in the ranges ($0° \leqslant a \leqslant 5°$) and ($0° \leqslant A \leqslant 10°$). D_o is calculated from the local time recorded for every observational scan. The brightness of the twilight is expressed in S_{10} units, which is the number of 10th magnitude stars of the solar type that gives the same brightness per one square degree as the object. Averages are always considered. The air mass $x(z)$ has been determined from the empirical formula of Eq. (1) of Young (Van De Hulst and Chamberlain 1957; Chamberlain, 1961). The following formulae (Eqs. (2) and (3)) are self-explained.

$$X(z) = \sec(a(1 - 0.0012\tan^2 a)) \quad (1)$$

$$Log\, I_1 = a_1 + b_1 X(z) \quad b_1 \equiv K, \tau = 2.303\ \mathrm{K} \quad (2)$$

$$S_{10} = 2.512^{10-C_\lambda} \quad (3)$$

where a is the altitude of the object, K is the extinction coefficient, C_λ is the reading of the multi-meter corresponding to a deviation of one deflection, τ is the optical thickness of the atmosphere, a_1 is a constant related to the aerosol content, while the transparency (P) of the atmosphere is given by Eq. (4).

$$P = e^{-\tau} \quad (4)$$

The brightness of twilight are determined from Eqs. (5) and (6).

$$I_1 = I_o e^{-x(z)} \quad (5)$$

$$m = m_o - 2.5x(z)log\, P \quad (6)$$

where m is the magnitude of the star inside the earth's atmosphere, and m_o is its magnitude outside, I_1 and I_o are the corresponding intensities (Hardie, 1962). Standard stars are observed during the night to determine the $x(z)$ and the optical depth τ then P.

It should be mentioned that the sun's depression (D_o) below the horizon has been determined according to the following relation (Roach and Gordon, 1973):

$$D_o = \sin^{-1}(\sin\varphi \sin\delta + \cos\varphi \cos\delta \cos H) \quad (7)$$

where φ is the latitude of the place, δ is the declination of the sun and H is the hour angle in degrees measured since solar noon.

3. Results

3.1. Transparency and extinction

The one-to-one correspondence between the color system of our scanner and international UBV and RGU is shown in paper I (Issa and Hassan, 2008a). The correlation coefficient approaches ($r > 0.98$) which indicates nearly perfect correspondence.

Figs. 1–3 show the relation between $log\, I_1$ and air mass $x(z)$ for standard stars observed at Matrouh (summer) along 4 nights dated June 1–5, 1984 using blue, yellow and red filters. The number of observed stars is 20 stars in the blue and the yellow and 13 in the red. The three figures show the results obtained for the site of observation, where least square solutions are used to determine the best fit. The slopes of the lines give the values of (K), the optical thickness (τ) and the intersection with the ($log\, I_1$ – axis) gives the values of $log\, I_o$ as it would be

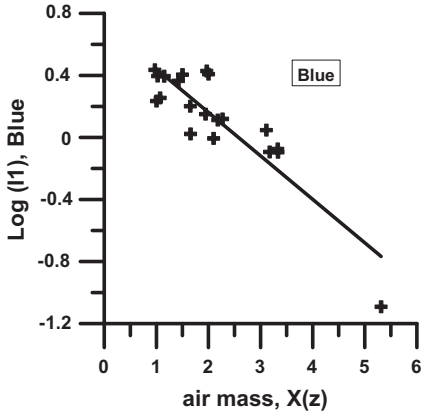

Fig. 1 The relation between $log(I_1)$ and $x(z)$ for blue color.

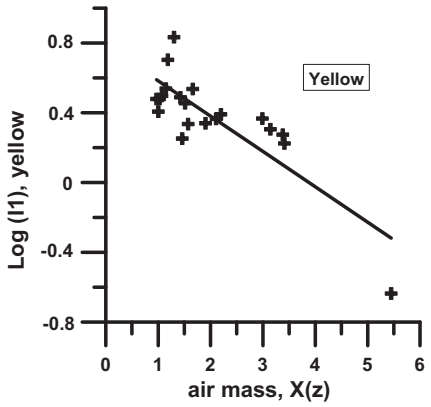

Fig. 2 The relation between $log(I_1)$ and $x(z)$ for yellow color.

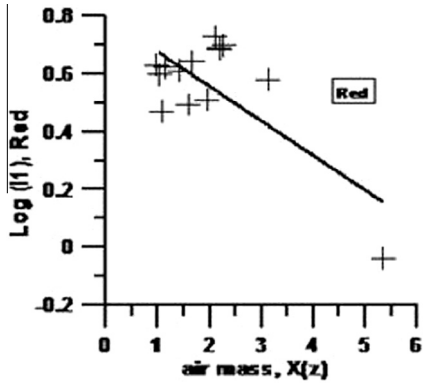

Fig. 3 The relation between $log(I_1)$ and $x(z)$ for red color.

outside the earth's atmosphere, where $z = 0$. Table 3 gives the deduced values of S_{10} in the B, V and R colors.

The values of Table 3 are multiplied by the relative measurements of sky night brightness deduced from Eqs. (1)–(4) to get the brightness in S_{10} units in the blue, yellow and red colors. Some scatter is shown in Figs. 1–3. This scatter is mainly due to instability of the atmospheric conditions. The effect of these instabilities can be noticed even during a single night. The extinction varies with direction in the sky. The variation is of particular interest during strong storms that occurred sometimes. The extinction is biggest in the blue, less in yellow, while its value is the lowest in red.

Applying Eqs. (2)–(4), the optical thickness (τ), extinction coefficient (K) and the mean values of the atmospheric transparency (P_λ) have been calculated in blue, yellow and red colors. The results are given in Table 4.

Table 4 indicates that Matrouh area is very turbid (the mean transparency is 0.64). The atmospheric transparency P_λ is fair for the red color (0.76) and accordingly the extinction coefficient is low (0.119). The extinction coefficient in the blue is therefore relatively 0.208. The coefficient of the atmospheric attenuation decreases with increasing wavelength, showing a general reddening. These results can be explained by the meteorological conditions of Tables 1 and 2, where the relative humidity has been 85.2% and the average temperature has been 18.9 °C. The increase in the temperature can cause an increase in the relative humidity which affects the optical thickness and, therefore, increases the extinction coefficient. The mean value of the transparency in the three colors is 0.64, indicating very turbid atmosphere in summer in Matrouh. Fig. 4 shows the relation between the optical thickness, the extinction coefficient and the transparency of the atmosphere against the wavelength for the three colors.

Table 3 The values of S_{10} (B, V, R) at Matrouh – June 1984.

Date	Blue	Yellow	Red
Summer (June)	1899	1632	1603

3.2. Results of twilight and discussion

For $A = 0°$ and $a = 5°$, 10°, 20°, 30°, 50°, the logarithm of the twilight brightness ($log\ B$) in S_{10} units is studied as a function of the depression of the sun below the horizon (D_o), in the B, V and R colors for both evening (E) and morning (M) twilights as shown in Figs. 5 and 6. The general trend of the twilight brightness with after sun's depression and before sun rise agrees well with the corresponding figures published by other investigators (Assad and Mikhail, 1967, 1974; Assad et al., 1977). Saturation of the curves starts to be observed at $D_o = 18°$ in the visual color. The curves start to bend at $D_o \approx 15°$ at different altitudes. However, especially at $a = 5°$ for morning twilight we expect the white thread becomes noticeable to the normal eye.

For evening twilight, most curves start to bend at $D_o \approx 16°$, while the tangent to the saturated part of curves and parallel to the D_o-axis cuts the brightness axis at $log\, S_{10}(R) \approx 3.5$, which is not far from that of morning twilight at $D_o \geqslant 18°$. On the other hand, for morning twilight, most curves start to bend at $D_o = 15°$, while the tangent to the saturated part of curves and parallel to the D_o-axis cuts the brightness axis at $log\, S_{10}(V) \approx 2.6$.

The solid lines parallel to the D_o-axis represent the normal eye threshold determined using the color transformation equations (Allen, 1973). Other set of lines especially in the red and visual colors for both evening and morning twilights are drawn exactly parallel to the D_o-axis and completely tangent to the

Table 4 The mean transparency P_λ (B, V, R), the extinction coefficient (K) and optical thickness (τ) at Matrouh for summer.

Blue			Yellow			Red		
τ	K	P	τ	K	P	τ	K	P
0.645	0.280	0.524	0.467	0.203	0.627	0.275	0.119	0.759

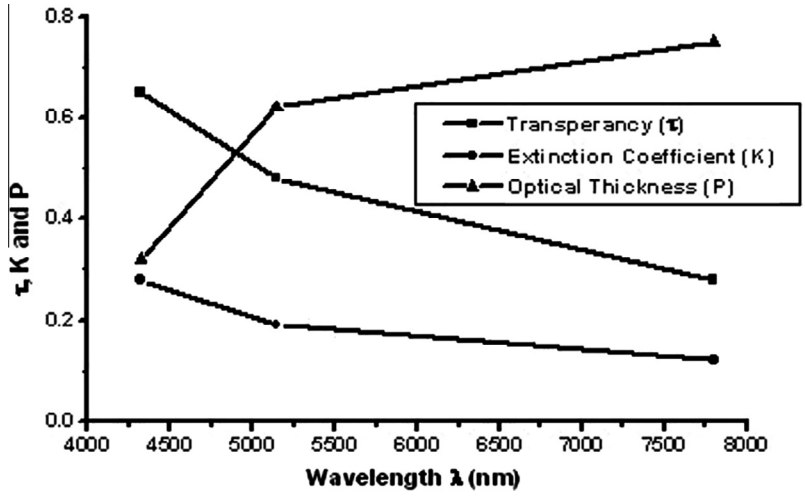

Fig. 4 The values of the Tao (τ), K and P for three colors.

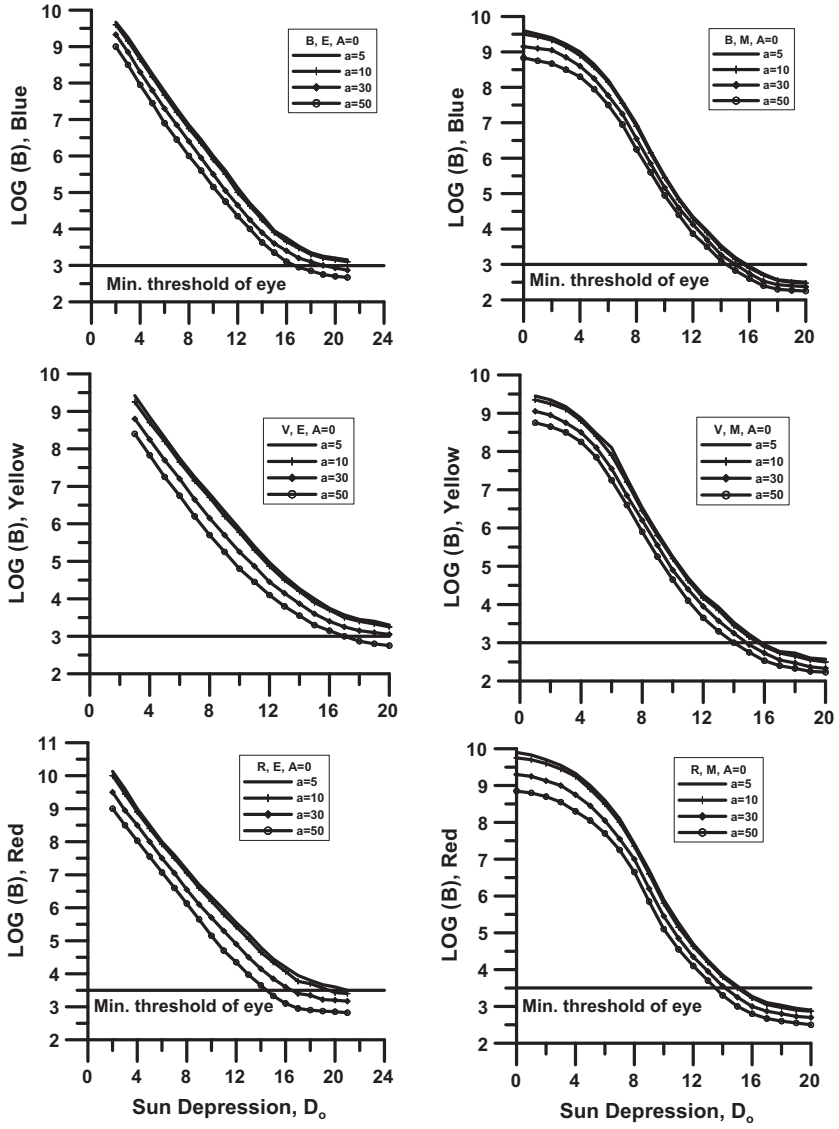

Fig. 5 The relation between $log\,B$ expressed in S_{10} (B, V, R) units with the sun's depression (D_o) at the site, for the evening (E) and morning (M) sky twilight at azimuth $A = 0°$ and at altitudes $a = 5°$, 10°, 30°, 50°, above the horizon.

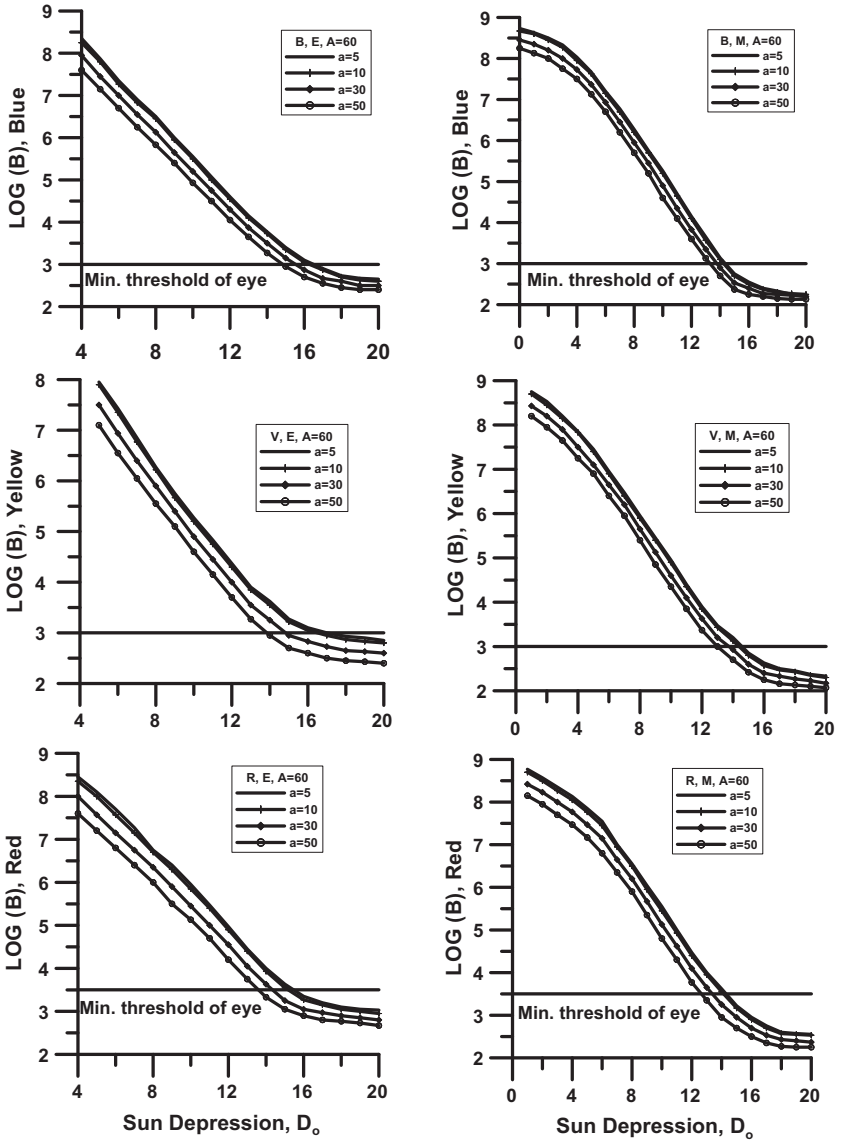

Fig. 6 The relation between $log\,B$ expressed in S_{10} (B, V, R) units with the sun's depression (D_o) at the site, for the evening (E) and morning (M) sky twilight at azimuth $A = 60°$ and at altitudes $a = 5°$, 10°, 30°, 50°, above the horizon.

saturation parts of the curves. They give 3.5 and 2.6 in $S_{10}(R)$ and $S_{10}(V)$ respectively. These values correspond to 4.25×10^{-16} J/cm^2 strad Å and 0.54×10^{-16} J/cm^2 strad Å respectively. These values are nearly equal to the eye threshold $(3.3–6.6) \times 10^{-16}$ J/cm^2 strad Å. Now, we are in a situation enabling us to assume that the threshold of the eye can announce the fall of the night after which the human eye can receive only photons from the background sky. Fig. 7 shows a comparison between the brightness of evening (E) and morning (M) in S_{10} units in the three colors; blue, yellow and red at $a = 5°$ with $A = 0°$ and $A = 60°$ in summer season. The comparison between both twilights shows that for $a = 5°$ and $A = 0°$ intersect each other nearly at $D_o \approx 8°$ and at $log\,S_{10}(B, V,$ and $R) \approx 7$. The other set of curves on the right hand side shows nearly no intersections but lying nearly very near to each other with very slight differences that we believe of no significance. The evening twilight curves lay however a little bit above the twilight morning curves. This could be interpreted as due to differences in atmospheric conditions.

3.3. Color index and twilight interval

Before approaching the horizon, the brightness of the sun decreases gradually with dramatic changes in its color. The short-wave length, the blue light, is dramatically scattered that the whole sky becomes blue, while the long wavelength passes through. Near the horizon and near the sun, the sky acquires yellow-orange colors, while the sky becomes pale on the horizon on the opposite side. Approaching more to the horizon, the disk of the sun becomes dark red. After sunset, the sky becomes orange-yellow which changes to green-azure in the upward direction. On the opposite horizon, a blue gray color prevails due to earth's shadow. More sinking of the sun below the horizon, the sky becomes deep-red, while a rose color as-

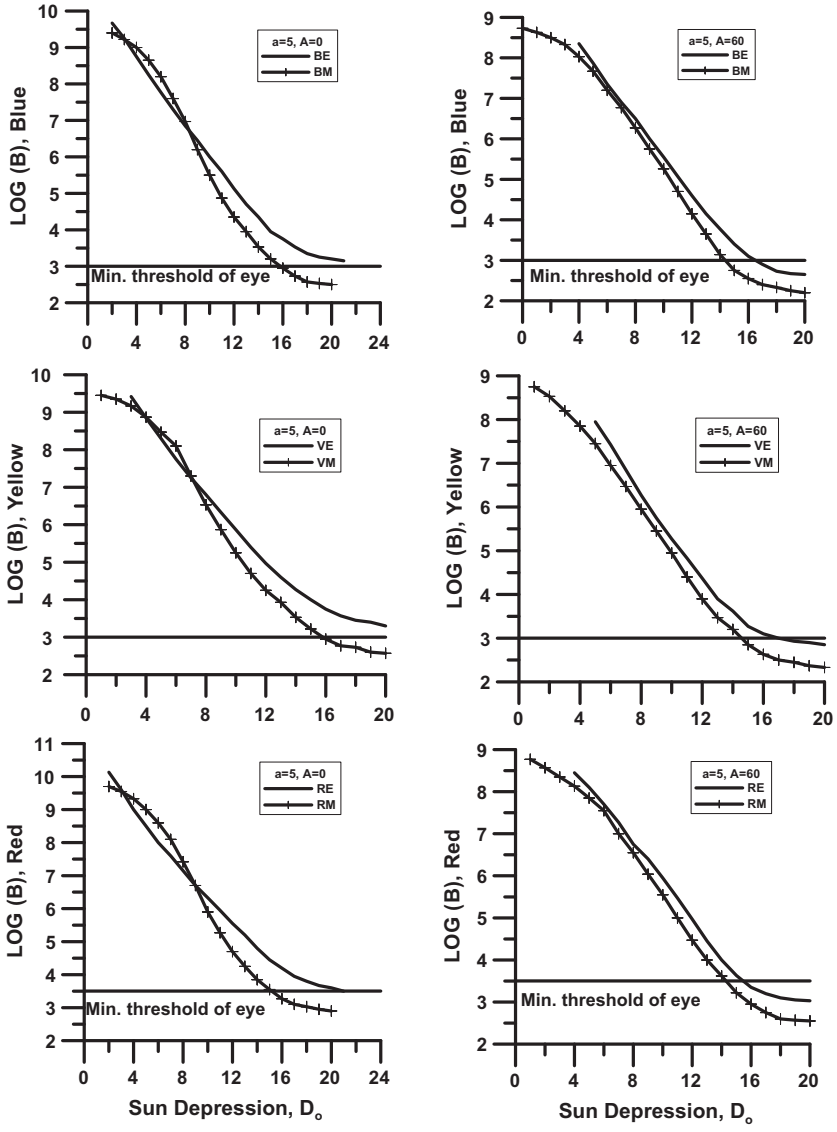

Fig. 7 A comparison between the brightness of evening (E) and morning (M) for in S_{10} unit in the three colors; blue, yellow and red at $a = 5°$ with $A = 0°$ and $A = 60°$ in summer season.

sumes itself at $a = 20$–$25°$. At the beginning of astronomical twilight, a pale-greenish white band appears.

With the above discussion in mind and religious statements regarding the end of twilight and its beginning, we can understand the dependence of the color indices on the sun's depression below the horizon.

Figs. 8 and 9 show the variations of the color indices (B–V), (B–R) and (V–R) as a function of the sun's depression D_o below the horizon for both evening and morning twilight. The first diagram in set 1 gives the trend of the values (B–V) against D_o. The values of (B–V) can be of positive, zero or negative values. If they are zero, then the B magnitudes are as big as the V magnitudes. This indicates that the amount of energy emitted in the blue color is as big as that in the visual (yellow) range. If $B > V$, then the amount of energy radiated in the visual range is bigger than in the blue. If $V > B$, the amount energy illuminating the sky in the blue is dominating and the sky tends to be blue. Accordingly, we can read the above mentioned variations in the figures. The positive values in (B–V) indicate $B > V$ so the visual illumination of the sky is dominating. As the difference becomes small, the blue illumination becomes bigger on account of the visual brightness. It continues till becoming equal at (B–V) = 0 at small depressions. After that, the scenery becomes reverse; the blue brightness becomes bigger on account of the visual until reaching maximum blue illumination at ($10° \leqslant D_o \leqslant 14°$). Then, it changes again in the opposite sense until becoming of equal effect on the sky around (B–V) = 0 at $D_o \geqslant 16°$. Then, again, visual illumination prevails all over the sky.

We are interested in red sky for Al-Eshaa prayer time. Saturation starts to show itself nearly at $D_o \geqslant 18°$ with a dominating visual illumination. We are looking for red sky according to the religious statement for the end of twilight. The (V–R) curves are all positive indicating $V > R$. Accordingly, the red

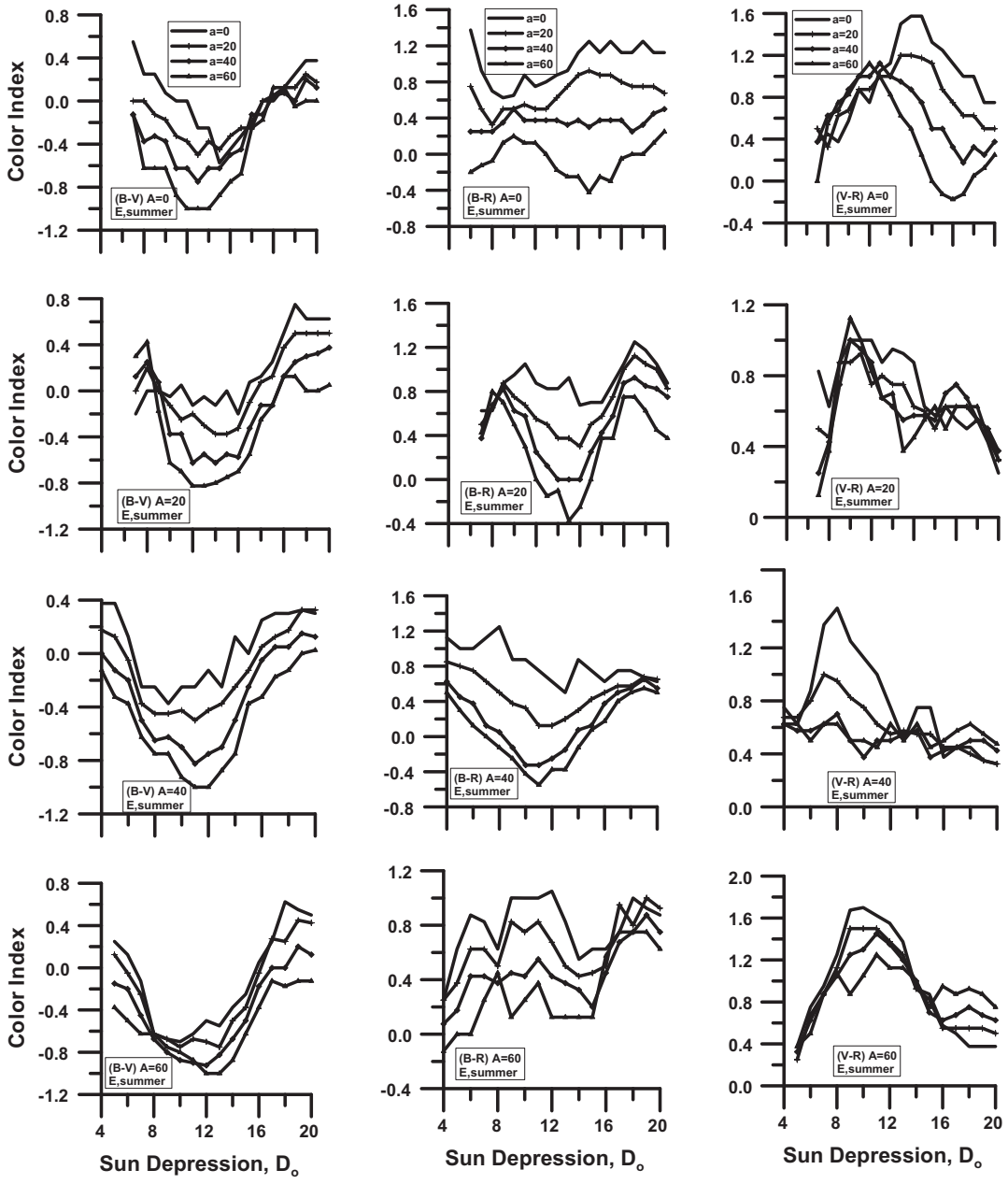

Fig. 8 The relation of the color index with D_o of evening twilight (E) at different altitudes (a) and azimuths (A) in summer.

illumination of the sky is dominating. The curves can show saturation starting nearly at $D_o \geqslant 18°$.

To summarize, we expect the end of twilight to be somewhere between ($18° \leqslant D_o \leqslant 20°$). The change in the three color sets indicates a continual increase toward a reddened sky for the end of twilight.

Our study has been continued for different altitudes till $a = 60°$ and azimuths to $A = 60°$. If we are dealing with prayer times in a certain area, we have to confine ourselves to the range ($0° \leqslant a \leqslant 5°$) and ($0° \leqslant A \leqslant 10°$).

For morning twilight, Fig. 8 comes in focus with the same sense of discussion about the evening twilight; we can read the color index curves of Fig. 9. For morning twilight, we are looking for a white light thread that can just be received by the normal typical eye. This corresponds to the early start (the bended part of the curve which we believe to be the dusk region). This occurs at ($14° \leqslant D_o \leqslant 16°$), which indicates dominating visual color.

For the end of twilight, we must rely on the religious statement translated nearly as: «*Twilight is reddening, if twilight sets, the end of twilight is in due time*» or «*The end of twilight is in due time if the twilight (the reddening) had just set*». The curves show a general saturation starting nearly at $D_o = 14°$ and continues till $D_o \geqslant 20°$. This indicates a general reddening as seen in the red color index curves in Figs. 8 and 9. The red threshold of the eye (3.5 S_{10}) and the religious fact of delaying the end of twilight as possible as we can lead us to assume the end of twilight whenever saturation starts to be leveled and

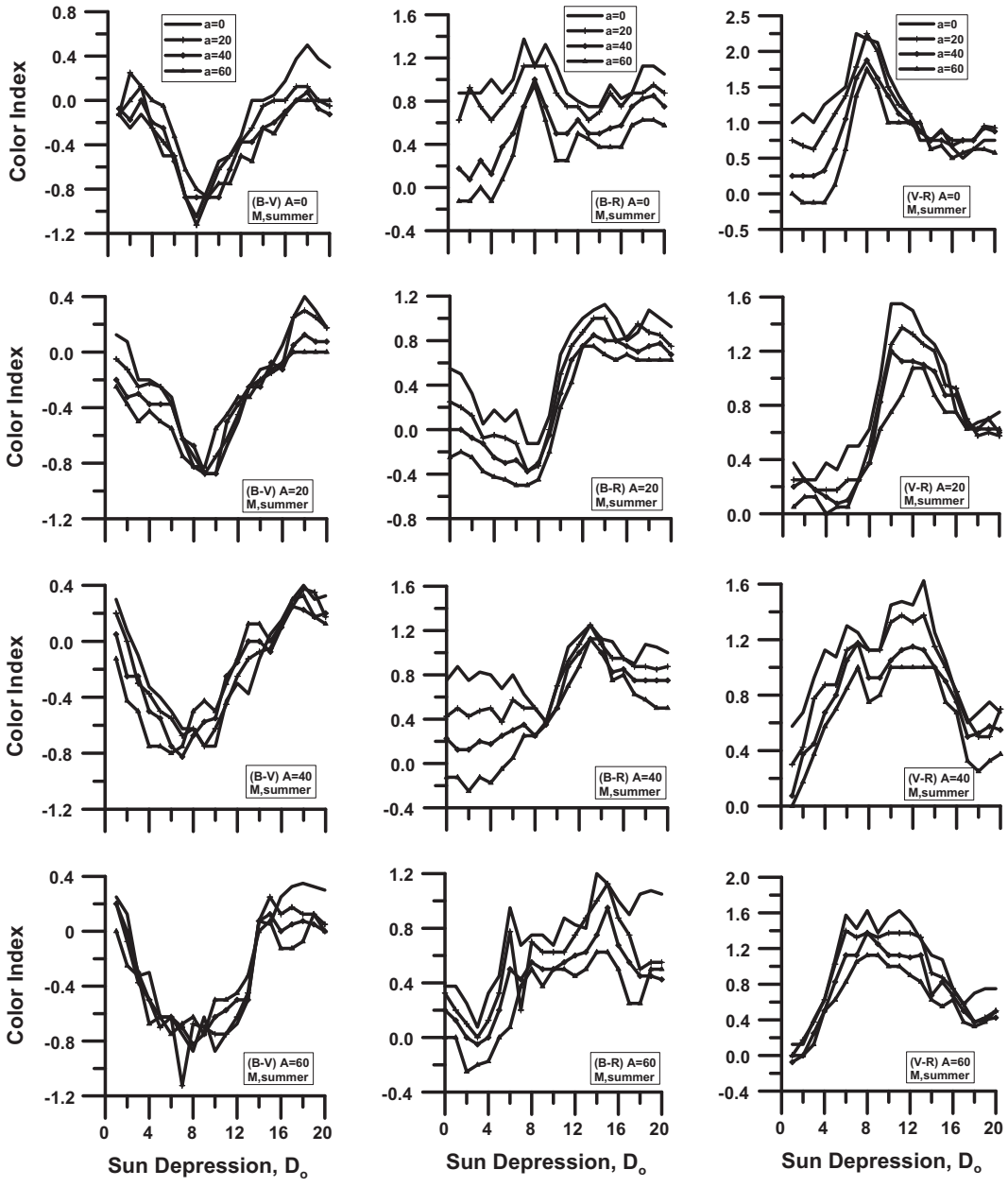

Fig. 9 The relation between the color index (B–V), (B–R) and (V–R) respectively and the sun depression angle D_o at different altitudes (a) and azimuths (A) of morning twilight.

parallel to the D_o-axis. This happens nearly at $D_o \approx 18$–$19°$. For the scientific studies, we have extended our observations to the range ($0° \leqslant a \leqslant 60°$) and ($0° \leqslant A \leqslant 60°$). Table 5 shows the color differences between evening and morning twilights as a function of D_o interpreted at each degree of depression. The curves show the brightness values are for $a = 5°$, $10°$, $30°$ and $50°$, while the values in between were obtained by interpolation.

3.4. Comparison

Comparing our color index variation with the sun depression to that given in Rosenberg's text (1966) about twilight Figs. (26) and (27), p. 37, we find a fairly good agreement. Rosenberg citing with the observation of Megrelishvili who has stated that «when the sun has dropped to 9–11° below the horizon, the blue coloration of the sky gives way to reddening». In our figures, the same can be deduced from set II as in Fig. 2, where we can read that at small depression ($4° \leqslant D_o \leqslant 8°$), the sky tends to be red, the reddening gets smaller as we go to bigger depression and, then, the sky gets blue again between ($8° \leqslant D_o \leqslant 12°$), where it starts to get reddened. Another comparison can be made with our study at Bahria oasis (Issa and Hassan, 2008c), which shows a strong agreement. It should be mentioned that the explanation given by Rosenberg has been done at the zenith as in his Fig. (26),

Table 5 Brightness values for both evening and morning twilights in the three colors given at each degree. The curves show the brightness values are for $a = 5°$ as an example, while the values in between were obtained by interpolation.

D_o	Evening (E)			Morning (M)		
	B	V	R	B	V	R
2	9.64		10.1	8.9	8.84	9.12
3	9.24	9.34	9.56	8.73	8.55	8.9
4	8.65	8.77	8.92	8.44	8.23	8.67
5	8.18	8.25	8.5	8.14	7.88	8.39
6	7.63	7.69	8.02	7.71	7.47	8.01
7	7.18	7.15	7.57	7.24	6.96	7.51
8	6.72	6.64	7.08	6.7	6.39	6.98
9	6.25	6.12	6.61	6.1	5.8	6.4
10	5.8	5.66	6.15	5.5	5.19	5.81
11	5.35	5.2	5.68	4.9	4.67	5.28
12	4.88	4.78	5.21	4.34	4.2	4.72
13	4.47	4.37	4.78	3.87	3.77	4.26
14	4.08	4.01	4.37	3.42	3.38	3.81
15	3.68	3.7	4.01	3.04	3.02	3.44
16	3.39	3.47	3.73	2.75	2.8	3.15
17	3.18	3.3	3.53	2.57	2.7	2.95
18	3.03	3.2	3.42	2.43	2.6	2.85
19	2.96	3.17	3.34	2.39	2.53	2.8

while in Fig. (27) it has been attained at $z = 70°$ and $A = 0°$. The general trend in Rosenberg (1966) curves tends to agree completely with ours.

Comparison between our published brightness and color index values for both twilights with Assad and Mikhail (1967, 1974) and Assad et al. (1977) shows a complete agreement.

4. Conclusion

For Matrouh in the summer we can conclude the following results:

1. Evening twilight ends in summer when the sun depression lies between ($18° \leqslant D_o \leqslant 20°$) if the minimum threshold of the eye in the red is 3.5 in S_{10} units for the red color. This happens at $a = 5°$ and $A = 10°$. It varies at other altitudes and azimuths. This value corresponds to 4.25×10^{-16} J/cm^2 strad Å.
2. The beginning of morning twilight announces its begin at ($18° \leqslant D_o \leqslant 20°$) and at $a = 5°$ and $A = 10°$. If we take the eye threshold to be 2.6 in S_{10} units for the blue and yellow colors, the dawn occurs at ($14° \leqslant D_o \leqslant 16°$). This value corresponds to 0.54×10^{-16} J/cm^2 strad Å.
3. The resulted values are nearly equal to the eye threshold agreed upon $(3.3–6.6) \times 10^{-16}$ J/cm^2 strad Å, which means that it can be considered as the end of the night after which the human eye starts to receive photons from the background sky, or as the begin of the night at which the human eye can receive only photons from the background sky.
4. The time interval from sunset to the end of evening twilight is bigger than that for the beginning of twilight if the threshold of the normal eye is considered.

References

Allen, C.W., 1973. Astrophysical Quantities, third ed. Athlon Press, London.

Assad, A.S., Mikhail, J.S., 1967. Brightness of the twilight and its variation and Misallat. Helwan Observatory Bulletin No. 68.

Assad, A.S., Mikhail, J.S., 1974. Atmospheric transparency at Misallat, Hellwan and Daraw. Helwan Observatory Bulletin No. 109.

Assad, A.S., Mikhail, J.S., Abdel Shaheed, S.N., 1977. Sky color variation during the twilight period at Helwan and Daraw. Helwan Observatory Bulletin No. 144.

Chamberlain, J.W., 1961. Physics of the Aurora and Air Glow vol. 2. Academic Press, New York and London.

Hardie, B.H., 1962. In: Hiltner, W.A. (Ed.), Astronomical Techniques. Univ. Chicago Press.

Issa, I.A., Hassan, A.H., 2008a. Transparency of the night sky at Bahria/Egypt, I. NRIAG Journal of Astronomy and Astrophysics (Special issue), 383–397, ISSN 1687-0980.

Issa, I.A., Hassan, A.H., 2008b. Evening and the beginning of twilights at Bahria/Egypt, II. NRIAG Journal of Astronomy and Astrophysics (Special issue), 399–411.

Issa, I.A., Hassan, A.H., 2008c. Eye criteria and times of end and begin of twilights at Bahria/Egypt, III. NRIAG Journal of Astronomy and Astrophysics (Special issue), 413–423.

Issa, I.A., Hassanin, N.Y., Hassan, A.H., Abdel-Hadi, Yasser A., 2011. Atmospheric transparency, twilight brightness and color indices at Kottamia of Egypt. NRIAG Journal of Astronomy and Astrophysics (Special issue), 379–398.

Roach, F.E., Gordon, J.L., 1973. The Light of the Night Sky. D. Reidel Publishing Company, USA.

Rosenberg, G.V., 1966. Twilight. Plenum Press, New York.

Van De Hulst, H.C., Chamberlain, J.W., 1957. Light Scattering by Small Particles. John Wiley Publishing Company, NY.